# The NMR Structure of the Pulmonary Surfactant-Associated Polypeptide SP-C in an Apolar Solvent Contains a Valyl-Rich α-Helix†

Jan Johansson,‡,§ Thomas Szyperski,‡ Tore Curstedt,‖ and Kurt Wüthrich*,‡

*Institut für Molekularbiologie und Biophysik, Eidenössiche Technische Hochschule-Hönggerberg, CH-8093 Zürich, Switzerland, and Department of Clinical Chemistry, Karolinska Institutet at Danderyd Hospital, S-182 88 Danderyd, Sweden*

*Received January 18, 1994*®

ABSTRACT: The nuclear magnetic resonance (NMR) structure of the pulmonary surfactant-associated lipopolypeptide C (SP-C) was determined in a mixed solvent of $C^2H_3Cl/C^2H_3OH$/0.1 M HCl 32:64:5 (v/v). Sequence-specific $^1H$ NMR assignments and the collection of conformational constraints were achieved with two-dimensional $^1H$ NMR, and the structure was calculated with the distance geometry program DIANA. The root mean square deviations for the well-defined polypeptide segment of residues 9–34 calculated for the 20 best energy-minimized DIANA conformers relative to their mean are 0.5 and 1.3 Å for the polypeptide backbone atoms N, $C^\alpha$, and C′, and for all heavy atoms, respectively. The 35-residue polypeptide chain of SP-C forms an α-helix between positions 9 and 34, which includes two segments of seven and four consecutive valyls that are separated by a single leucyl residue. The N-terminal hexapeptide segment, which includes two palmitoylcysteinyls, is flexibly disordered. The length of the α-helix is about 37 Å, and the helical segment of residues 13–28, which contains exclusively aliphatic residues with branched side chains, is 23-Å long and about 10 Å in diameter. The α-helix is outstandingly regular, with virtually identical $\chi^1$ angles for all valyl residues. The observation of a helical structure of SP-C was rather unexpected, considering that Val is generally underrepresented in α-helices, and it provides intriguing novel insights into the structural basis of SP-C functions as well as into general structural aspects of protein–lipid interactions in biological membranes.

The pulmonary-surfactant-associated lipopolypeptide C (SP-C)[1] is a highly hydrophobic 4.2 kDa lipopeptide, where the C-terminal two thirds of the 35-residue polypeptide chain consist almost exclusively of branched-chain aliphatic residues, including stretches of up to seven consecutive valyls (Johansson et al., 1988a,b). Furthermore, palmitoyl groups are thioester-linked to each of the two Cys residues at positions 5 and 6 in human and porcine SP-C (Curstedt et al., 1990). The hydrophobic C-terminal part of the polypeptide chain is highly conserved between different species, while the more hydrophilic N-terminal part exhibits some variance, including replacement of one of the palmitoylcysteinyls by phenylalanine in canine SP-C (Johansson et al., 1991). The secondary structure content and the orientation of SP-C incorporated into phospholipid bilayers have been studied by infrared spectroscopy (Pastrana et al., 1991; Vandenbussche et al., 1992), and $^2H$ nuclear magnetic resonance (NMR) studies of selectively deuterated, SP-C-containing 1,2-dipalmitoyl-*sn*-glycero-3-phosphocholine (DPPC) bilayers indicated that the positive charges in the N-terminal dodecapeptide segment of SP-C are located near the lipid bilayer surface (Morrow et al., 1993). However, due to the pronounced hydrophobicity of SP-C and the ensuing difficulties in preparing either suitable crystals for X-ray diffraction measurements or solutions for NMR spectroscopy, no atomic resolution structure has previously been reported. The present paper describes an NMR structure determination of native SP-C in a mixed solvent of chloroform, methanol, and 0.1 M hydrochloric acid 32:64:5 (v/v).

A structure determination of SP-C is of general interest with regard to further studies of protein–lipid interactions in biological membranes as well as in connection with the biological role of this lipopolypeptide in pulmonary surfactant, which is a complex mixture of phospholipids and the four surfactant-associated proteins SP-A, SP-B, SP-C, and SP-D. Pulmonary surfactant is primarily needed for reducing the surface tension at the alveolar air/liquid interface (for recent reviews see Johansson et al. (1994) and Robertson et al. (1992)), and in premature infants surfactant deficiency is associated with respiratory distress syndrome (RDS). Exogenous surfactant used for treatment of this potentially lethal disease contains in addition to phospholipids, especially DPPC, small amounts of two of the surfactant-associated polypeptides, SP-B and SP-C (Collaborative European Multicenter Study Group, 1988). These appear to be important for the formation and stability of surface-active DPPC monolayers at the air/liquid interface by facilitating rapid interconversion between different phases adopted by surfactant *in vivo* and by selectively removing lipid species from initially formed monolayers (Curstedt et al., 1987; Hawgood et al., 1987; Yu & Possmayer, 1990; Simatos et al., 1990; Oosterlaken-Dijksterhuis et al.,

† This work was supported by the Schweizerischer Nationalfonds (Project 31.32033.91), the Swedish Medical Research Council (Grants 13X-10371 and 13F-10245), the Axel Tielman Fund, the Oscar II:s Fund, the Swedish Institute, the Foundation Blanceflor Boncompagni-Ludovisi, née Bildt, and the Swedish Society of Medicine.

‡ Eidgenössische Technische Hochschule-Hönggerberg.

§ Present address: Department of Medical Biochemistry and Biophysics, Karolinska Institutet, S-171 77 Stockholm, Sweden.

‖ Karolinska Institutet at Danderyd Hospital.

® Abstract published in *Advance ACS Abstracts,* April 1, 1994.

[1] Abbreviations: SP, surfactant protein: DPPC, 1,2-dipalmitoyl-*sn*-glycero-3-phosphocholine; RDS, respiratory distress syndrome; NMR, nuclear magnetic resonance; 2QF-COSY, two dimensional two-quantum filtered correlation spectroscopy; TOCSY, two-dimensional total correlation spectroscopy; NOE, nuclear Overhauser enhancement; NOESY, two-dimensional nuclear Overhauser enhancement spectroscopy; ROESY, two-dimensional nuclear Overhauser enhancement spectroscopy in the rotating frame; TSP, trimethylsilyl [2,2,3,3-$^2H_4$]propionate; RMSD, root mean square deviation.

0006-2960/94/0433-6015$04.50/0 

1991a,b; Horowitz et al., 1992). On a practice-minded vein, a structural basis that could provide a rationale for these varied, important functional roles of SPs might also serve as a platform for future design of improved exogenous surfactant for treatment of RDS.

## MATERIALS AND METHODS

*Protein Purification.* Native SP-C was purified as described by Curstedt et al. (1987): Minced pig lungs were washed with saline, and after centrifugation the supernatant was extracted with chloroform/methanol 2:1 (v/v). Phospholipids and hydrophobic proteins were then isolated by reverse-phase chromatography of the extract on Lipidex-5000 in ethylene chloride/methanol 1:4 (v/v). From the resulting mixture, SP-C was eventually separated from SP-B and phospholipids by Sephadex LH-60 chromatography in chloroform/methanol/0.1 M HCl 19:19:2 (v/v). Quantitative amino acid analysis of the samples revealed only trace amounts of amino acids not present in the SP-C polypeptide chain, verifying the absence of contaminating proteins.

*NMR Sample Preparations.* Samples of native SP-C were prepared by dissolving 2.2 or 4.4 mg of the dried lipopolypeptide either in 500 μL of $C^2HCl_3/C^2H_3OH$/0.1 M HCl 32:64:5 (v/v) or in 500 μL of $C^2HCl_3/C^2H_3O^2H$/0.1 M $^2$HCl 32:64:5 (v/v), giving final SP-C concentrations of about 1.1 or 2.2 mM, respectively. The samples were kept at 4 °C between different NMR measurements.

For NMR experiments with pure lipid, 27 mg of palmitic acid methyl ester (Sigma Chemicals) was dissolved in 500 μL of $C^2HCl_3/C^2H_3O^2H$/0.1 M $^2$HCl 32:64:5 (v/v), resulting in an approximate concentration of 0.2 M.

*NMR Measurements.* Two-dimensional $^1$H NMR spectra were recorded on Bruker AMX 500 or AMX 600 spectrometers in the pure-phase absorption mode using the States-TPPI method (Marion et al., 1989b). The spectra were processed using the program PROSA (Güntert et al., 1992). The $^1$H chemical shifts were calibrated relative to trimethylsilyl [2,2,3,3-$^2H_4$]propionate (TSP). All $^1$H NMR spectra of SP-C (Table 1) were recorded at 600 MHz and 10 °C, and the 2QF-COSY spectrum of the palmitoyl methyl ester was recorded at 500 MHz and 10 °C. The residual water signal after preirradiation was further reduced using the convolution method of Marion et al. (1989a). Before Fourier transformation the time domain data were zero-filled and multiplied with shifted sine-bell window functions (DeMarco & Wüthrich, 1976). The spectra were baseline-corrected in both dimensions using the FLATT routine (Güntert & Wüthrich, 1992). Vicinal scalar coupling constants $^3J_{NH\alpha}$ were determined from the NOESY spectrum in the protonated solvent by inverse Fourier transformation of in-phase multiplets (Szyperski et al., 1992a).

*Software Used for the Structure Calculation.* The cross peaks of the NOESY spectra of native SP-C (Table 1) were integrated using the program EASY (Eccles et al., 1991), and the resulting NOE intensities were converted to upper distance limits with the program CALIBA (Güntert et al., 1991a). Dihedral angle constraints based on intraresidual and sequential NOE connectivities and on the scalar coupling constants $^3J_{NH\alpha}$ were generated using the program HABAS (Güntert et al., 1989). Structure calculations were performed with the program DIANA (Güntert et al., 1991a,b), using one REDAC cycle (Güntert & Wüthrich, 1991) with the maximal target function value per residue for locally acceptable segments set to 0.4 Å$^2$. Stereospecific assignments for pairs of diastereotopic substituents were obtained with the program

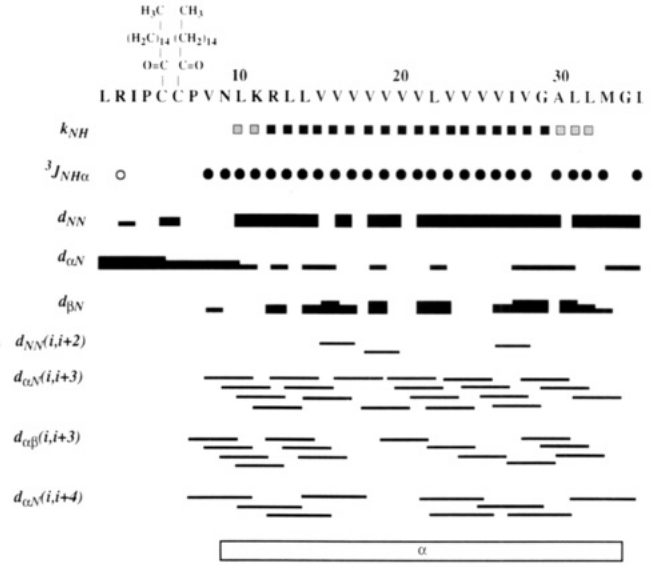


FIGURE 1: Amino acid sequence of porcine SP-C with palmitoylcysteinyls in positions 5 and 6 and survey of sequential and medium-range NOE connectivities, of slowly exchanging amide protons and of small and large $^3J_{NH\alpha}$ coupling constants. In the row $k_{NH}$, filled boxes identify residues with amide proton exchange rates $< 2.7 \times 10^{-4}$ min$^{-1}$, and dotted boxes, those with $2.7 \times 10^{-4} < k_{NH} < 8.3 \times 10^{-4}$ min$^{-1}$. For all other residues we estimated that $k_{NH} > 1 \times 10^{-2}$ min$^{-1}$ (see text for details). In the row $^3J_{HN\alpha}$, filled and open circles denote residues with $^3J_{NH\alpha} < 5.0$ Hz and $^3J_{NH\alpha} > 8.0$ Hz, respectively, with all other $^3J_{NH\alpha}$ coupling constants between 6.0 and 8.0 Hz. The following three rows present the sequential connectivities $d_{NN}$, $d_{\alpha N}$ and $d_{\beta N}$ ($d_{N\delta}$, $d_{\alpha\delta}$ and $d_{\beta\delta}$ for Xxx–Pro), where the height of the bar reflects the NOE intensity. The medium-range connectivities $d_{NN}(i,i+2)$, $d_{\alpha N}(i,i+3)$, $d_{\alpha\beta}(i,i+3)$, and $d_{\alpha N}(i,i+4)$ are represented by lines starting and ending at the positions of the interacting residues. The sequence location of the α-helix identified from the structure calculation with the program DIANA using all experimental constraints is indicated at the bottom.

GLOMSA (Güntert et al., 1991a,b). Energy minimization of the DIANA conformers was performed *in vacuo* using a modification of the AMBER force field (Weiner et al., 1986) implemented in the program OPAL (P. Luginbühl, P. Güntert, M. Billeter, and K. Wüthrich, to be published), where distance constraints and dihedral angle constraints are included as pseudoenergy terms calibrated so that violations of 0.1 Å or 2.5°, respectively, correspond to an energy of $kT/2$ at room temperature (Billeter et al., 1990). Analyses of the results of the structure calculations in terms of hydrogen bond identification, RMSD values, dihedral angle distributions, and visual comparisons of different individual conformers were performed using the program XAM (Xia, 1992).

## RESULTS AND DISCUSSION

*NMR Assignments.* Sequence-specific $^1$H NMR assignments were obtained using standard procedures for small proteins (Wüthrich, 1986), with computer support by the program EASY (Eccles et al., 1991). Due to the uneven distribution of amino acid types in the sequence of SP-C (Figure 1), there was extensive overlap in the homonuclear $^1$H NMR spectra, which were used because only the natural polypeptide at natural isotope distribution was available for this study. To document that nearly complete $^1$H NMR assignments could nonetheless be obtained, Figures 2–4 show three of the two-dimensional $^1$H NMR spectra used. From the TOCSY spectrum of Figure 2 and a 2QF-COSY spectrum obtained under identical conditions, all 13 Val spin systems were found, and the spin systems of the unique Lys 11 and Ala 30, the pairs of Arg and Gly residues in positions 2 and

Table 1: Survey of the Two-Dimensional [$^1$H,$^1$H] NMR Spectra Recorded ($T$ = 10 °C)

| sample | experiment[a] | $\tau_m$[b] | data matrix[c] | $t_{1max}$[d] | $t_{2max}$[d] | $t_{tot}$[e] | res[f] |
|---|---|---|---|---|---|---|---|
| 2.2 mM native SP-C in $C^2HCl_3$/ $C^2H_3OH$/0.1 M HCl 32:64:5 | 2QF-COSY | | 512 × 1400 | 85 | 254 | 12 | 5.9/2.0 |
| | clean-TOCSY | 80 | 480 × 1400 | 80 | 254 | 24 | 5.9/2.0 |
| | NOESY | 50 | 200 × 1400 | 33 | 254 | 10 | 5.9/2.0 |
| 1.1 mM native SP-C in $C^2HCl_3$/ $C^2H_3OH$/0.1 M HCl 32:64:5 | ROESY | 25 | 427 × 1024 | 71 | 127 | 25 | 5.9/2.0 |
| 2.2 mM native SP-C in $C^2HCl_3$/ $C^2H_3O^2H$/0.1 M $^2$HCl 32:64:5 | clean-TOCSY | 60 | 152 × 1400 | 39 | 291 | 6 | 5.2/1.7 |
| | NOESY | 50 | 420 × 1400 | 78 | 291 | 22 | 5.2/1.7 |
| 0.2 M palmitoyl methyl ester in $C^2HCl_3$/ $C^2H_3O^2H$/0.1 M $^2$HCl 32:64:5 | 2QF-COSY | | 1024 × 1024 | 170 | 170 | 2 | 5.9/1.5 |

[a] References for the experimental schemes used are 2QF-COSY (Rance et al., 1983), clean-TOCSY (Griesinger et al., 1988), NOESY (Anil-Kumar et al., 1980), and ROESY (Bothner-By et al., 1984). [b] Mixing time in milliseconds. [c] Size of the acquired data matrices in complex points. [d] Maximal $t_1$ and $t_2$ values, respectively, in milliseconds. [e] Approximate total measuring time in hours. [f] Spectral resolution after zero-filling along $\omega_1/\omega_2$ in Hz/point.

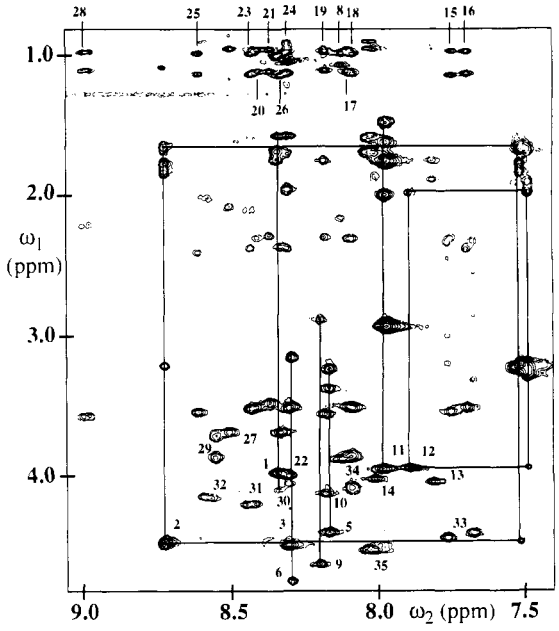


FIGURE 2: Contour plot of a 600-MHz clean-TOCSY spectrum of a 2.2 mM solution of native SP-C in the mixed solvent $C^2HCl_3$/ $C^2H_3OH$/0.1 M HCl (see Table 1 for parameters used). The spectral region ($\omega_1$ = 0.8–4.8 ppm, $\omega_2$ = 7.4–9.1 ppm) is shown, which contains the cross peaks of the $\alpha$-protons and aliphatic side chain protons with the amide protons. In the bottom half of the figure, the cross peaks correlating the backbone $\alpha$- and amide protons of the non-valyl residues have been labeled in the spectrum with the corresponding residue number. The long vertical lines connect the protons of the seven non-glycyl residues that served as starting points for the sequential assignment procedure (see text), where for Arg 2 and Arg 12 the connectivities to the $\epsilon$-proton (see Table 2 for the chemical shifts) have also been drawn. The short vertical lines at the top identify the amide proton chemical shifts of the 13 Val residues, as indicated by the sequence positions.

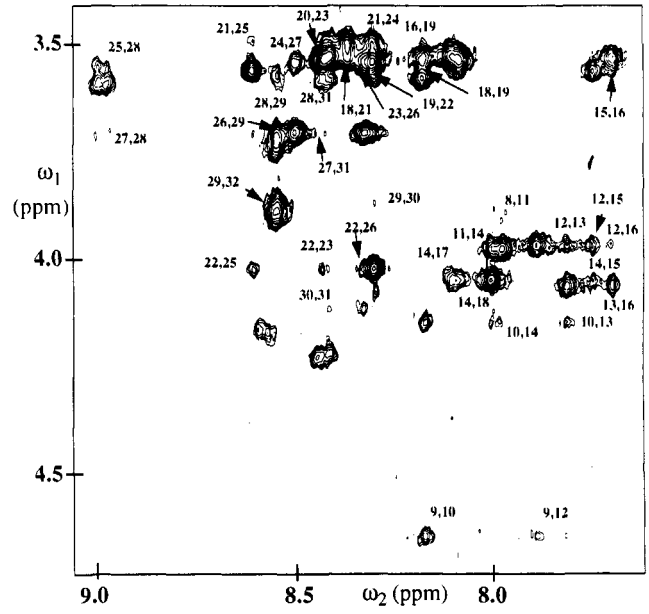


FIGURE 3: Spectral region ($\omega_1$ = 3.4–4.8 ppm, $\omega_2$ = 7.6–9.1 ppm) of the 600-MHz NOESY spectrum of a 2.2 mM solution of native SP-C in $C^2HCl_3$/$C^2H_3O^2H$/0.1 M $^2$HCl (see Table 1), which contains the $\alpha$-proton–amide proton cross peaks. Sequential and medium-range $\alpha$-proton–amide proton connectivities (Figure 1) are labeled with the sequence locations of the interacting residues, where the first number refers to the residue interacting with C$^\alpha$H. Unlabeled peaks correspond to intraresidual $d_{\alpha N}(i,i)$ peaks (for the notation used see Wüthrich (1986)).

12, and 29 and 34, respectively, and the three AMX spin systems of the C$^\alpha$H–C$^\beta$H$_2$ fragments of Cys 5, Cys 6, and Asn 9 could be unambiguously identified. Asn 9 could subsequently be distinguished from the other two AMX spin systems by its $\beta$-proton–side chain amide proton NOE connectivities (Wüthrich, 1986). The nine spin systems, which either are unique or occur only twice in porcine SP-C (Johansson et al., 1988a), then served as reference points for the sequential assignment procedure. Figures 3 and 4 show the $d_{\alpha N}$ and $d_{NN}$ regions, respectively, of the NOESY spectrum recorded in $C^2HCl_3$/$C^2H_3O^2H$/0.1 M $^2$HCl after complete exchange of the amide protons of residues 1–9 and 33–35, which was particularly helpful for obtaining the $d_{NN}$ assignments (Figure 4). In spite of the large number of consecutive Val residues (Figure 1) the chemical shift dispersion of the backbone amide protons was sufficient to obtain sequential connectivities for most of the Val–Val segments from $d_{NN}$ connectivities, and in addition several of the $d_{\alpha N}$ and $d_{\beta N}$ connectivities were also identified (Figure 1). Visual inspection of the cross peak line shapes was important for obtaining many of these assignments.

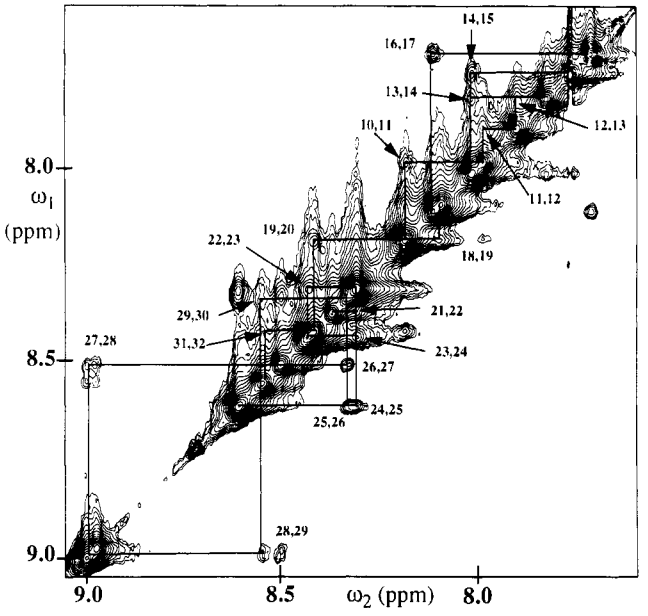


FIGURE 4: Spectral region ($\omega_1$ = 7.6–9.1 ppm, $\omega_2$ = 7.6–9.1 ppm) of the same 600-MHz NOESY spectrum of native SP-C as in Figure 3, which contains the amide proton–amide proton cross peaks. The sequential $d_{NN}$ cross peaks found for the polypeptide segment 10–30 are connected with lines and identified with the sequence positions of the connected residues.

The identification of the following connectivities presented special difficulties: The chemical shifts of the amide protons of Leu 22 and Val 24 are degenerate so that the $d_{NN}$ connectivities 22–23 and 23–24 are exactly overlapped. The corresponding NOESY cross peak has about twice the volume of peaks from non-overlapped $d_{NN}$ connectivities (Figure 4), suggesting that both $d_{NN}$ connectivities are indeed present. For the pairs of neighboring residues Val 17–Val 18 and Val 20–Val 21, the near-identity of the chemical shifts (Table 2) precluded the identification of sequential NOEs (Figure 1). However, since the intervening segment 18–20 is firmly established (Figure 1), the spin systems of all residues could eventually be assigned. Overall, except for the γ-methine resonances of Leu 1, 10, 13, 14, and 35, which are possibly overlapped with one of the β-methylene proton resonances, the ε-methyl group of Met 33, and the fact that only one NMR line was found for some pairs of methylene protons and isopropyl methyls, all $^1$H resonances of native SP-C have been assigned (Table 2).

The chemical shifts of the palmitoyl groups which are thioester-linked to Cys 5 and Cys 6 (Curstedt et al., 1990) were obtained from the 2QF-COSY and TOCSY spectra. Since there are no cross peaks between the acyl-chain protons and other protons of the palmitoylcysteinyls in these spectra, an indirect approach using $^1$H chemical shifts measured in the 2QF-COSY spectrum of the palmitoyl methyl ester in $C^2HCl_3/C^2H_3O^2H$/0.1 M $^2$HCl (Table 1) was used. These

Table 2: Proton Chemical Shifts (ppm) of Native SP-C[a]

| residue | NH | αH | βH | others |
|---|---|---|---|---|
| Leu1 | 8.34 | 3.99 | 1.69, 1.75 | δCH$_3$ 1.01, 1.03 |
| Arg2 | 8.72 | 4.49 | 1.78, 1.84 | γCH$_2$ 1.66; δCH$_2$ 3.23; εNH 7.51 |
| Ile3 | 8.30 | 4.51 | 1.96 | γCH$_2$ 1.22, 1.65; γCH$_3$ 1.06; δCH$_3$ 0.95 |
| Pro4 | | 4.44 | *2.03, 2.28* | γCH$_2$ 2.09; δCH$_2$ 3.74, 3.97 |
| Cys5[b] | 8.16 | 4.42 | 3.26, 3.28 | C$^2$H$_2$ 2.62; C$^3$H$_2$ 1.67; C$^{4-15}$H$_2$ 1.34; CH$_3$ 0.90 |
| Cys6[b] | 8.29 | 4.77 | *3.17, 3.52* | C$^2$H$_2$ 2.34; C$^3$H$_2$ 1.62; C$^{4-15}$H$_2$ 1.32; CH$_3$ 0.90 |
| Pro7 | | 4.43 | 2.11, 2.35 | γCH$_2$ 2.18; δCH$_2$ 3.88, 3.95 |
| Val8 | 8.12 | 3.90 | 2.17 | γCH$_3$ 1.00, 1.08 |
| Asn9 | 8.19 | 4.64 | 2.90 | δNH$_2$ *7.81, 7.12* |
| Leu10 | 8.18 | 4.14 | 1.76 | δCH$_3$ 0.96, 1.02 |
| Lys11 | 7.98 | 3.97 | 2.00 | γCH$_2$ 1.49, 1.63; δCH$_2$ 1.76; εCH$_2$ 2.95; ζNH$_2$ 7.97 |
| Arg12 | 7.89 | 3.96 | 2.00 | γCH$_2$ 1.69, 1.92; δCH$_2$ 3.26, 3.29; εNH 7.48 |
| Leu13 | 7.81 | 4.06 | 1.76, 1.89 | δCH$_3$ 0.96 |
| Leu14 | 8.01 | 4.05 | *1.75, 1.88* | δCH$_3$ 0.97 |
| Val15 | 7.75 | 3.56 | 2.31 | γCH$_3$ *0.98, 1.15* |
| Val16 | 7.69 | 3.53 | 2.39 | γCH$_3$ *0.99, 1.15* |
| Val17 | 8.10 | 3.51 | 2.32 | γCH$_3$ 0.97, 1.13 |
| Val18 | 8.08 | 3.54 | 2.32 | γCH$_3$ *1.00, 1.14* |
| Val19 | 8.17 | 3.57 | 2.30 | γCH$_3$ 0.98, 1.12 |
| Val20 | 8.40 | 3.52 | 2.31 | γCH$_3$ 0.97, 1.13 |
| Val21 | 8.36 | 3.49 | 2.29 | γCH$_3$ *0.97, 1.13* |
| Leu22 | 8.30 | 4.02 | *1.93, 1.98* | γH 1.70; δCH$_3$ 0.92 |
| Val23 | 8.43 | 3.54 | 2.38 | γCH$_3$ *1.00, 1.15* |
| Val24 | 8.30 | 3.53 | 2.39 | γCH$_3$ 0.99, 1.14 |
| Val25 | 8.61 | 3.56 | 2.42 | γCH$_3$ *1.00, 1.14* |
| Val26 | 8.33 | 3.70 | 2.37 | γCH$_3$ *1.00, 1.15* |
| Ile27 | 8.50 | 3.70 | 2.09 | γCH$_2$ 1.17, 1.95; γCH$_3$ 0.96; δCH$_3$ 0.87 |
| Val28 | 8.97/9.00 | 3.59 | 2.22 | γCH$_3$ *0.99, 1.12* |
| Gly29 | 8.55 | *3.73, 3.88* | | |
| Ala30 | 8.30/8.34 | 4.07/4.11 | 1.58 | |
| Leu31 | 8.42/8.45 | 4.22 | 2.00, 2.11 | γH 1.59; δCH$_3$ 0.96 |
| Leu32 | 8.57/8.59 | 4.17/4.16 | 2.03 | γH 1.49; δCH$_3$ 0.92 |
| Met33 | 7.67/7.76 | 4.43/4.46 | 2.34/2.35<br>2.57/2.46 | γCH$_2$ 2.87/3.01, 3.33/3.21 |
| Gly34 | 8.09 | 3.88, 4.10 | | |
| Leu35 | 8.02 | 4.55 | 1.60, 1.70 | δCH$_3$ 0.92, 0.97 |

[a] The chemical shifts relative to TSP are for native SP-C solubilized in $C^2HCl_3/C^2H_3OH$/0.1 M HCl 32:64:5 (v/v) at 10 °C. For methylene and isopropyl groups two chemical shifts are given only when two resonance lines could be identified, and the stereospecific assignments are given as far as they could be established. The chemical shifts are then printed in italics, and the first value is the shift of the proton and the lower branch number, *e.g.*, the $\beta^2$ proton or the $\gamma^1$ methyl of Val. For the residues 28 and 30–33, two sets of chemical shifts were observed (see text). The values listed first belong to one molecular species; the second values belong to the other one. [b] The palmitoyl groups could not be sequentially assigned (see text). The numeration of the methylene groups is such that $C^2$ is covalently linked to the carbonyl carbon.

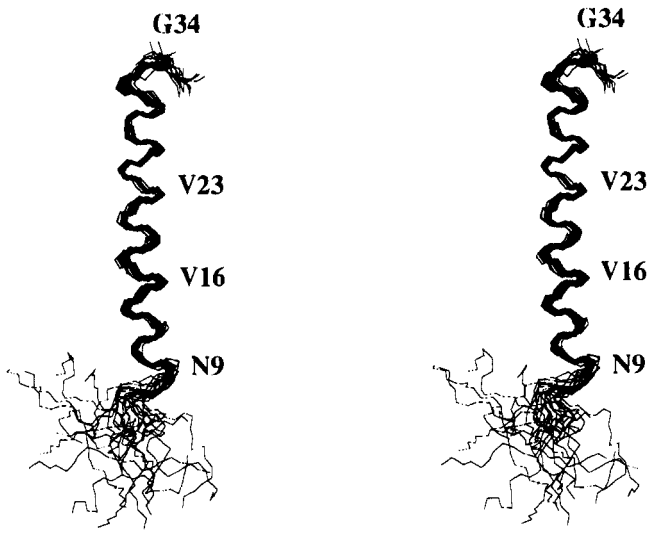


FIGURE 5: Stereoview of the polypeptide backbone of the 20 final, energy-refined DIANA conformers of native SP-C used to represent the NMR structure in solution. The individual conformers 2–19 have been superimposed with conformer 1 for pairwise minimum RMSD of the backbone atoms N, $C^{\alpha}$, and C′ of residues 7–34. Some amino acid residues are identified with the one-letter amino acid code and the sequence location.

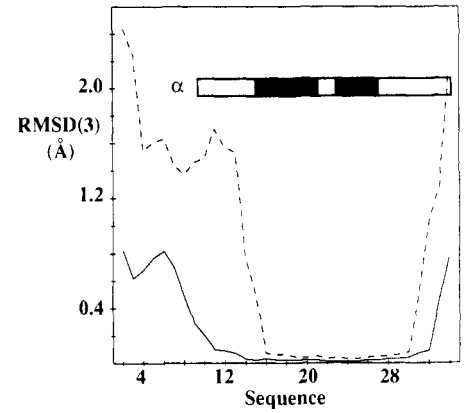


FIGURE 6: Plots of the average of the pairwise local RMSD values, RMSD(3), for the 20 best energy-refined conformers to the mean structure *versus* the amino acid sequence. The values are calculated for three-residue segments and plotted for the middle residue of each segment: solid line, backbone atoms N, $C^{\alpha}$, and C′; dashed line, all heavy atoms. The box labeled α identifies the location of the α-helix, where the two stretches of Val residues (Figure 1) are indicated by shaded blocks.

"random coil" chemical shifts of $C^2H_2$, $C^3H_2$, $C^{4-15}H_2$, and $C^{16}H_3$ (see Table 2 for the nomenclature) are respectively 2.35, 1.64, 1.34, and 0.92 ppm. The spectra of native SP-C were then searched for peaks with chemical shifts similar to those of the palmitoyl methyl ester which did not belong to any of the amino acid spin systems. Two palmitoyl spin systems were thus identified, which differ significantly only in the chemical shifts of $C^2H_2$ (Table 2). Since no palmitoyl–polypeptide NOEs were found either in the ROESY or the NOESY spectra, indicating that the absence of NOEs is not simply related to unfavorable effective correlation times, the two palmitoyl groups could not be individually assigned.

Met 33 exhibits two sets of resonances, which differ in the chemical shifts of all protons (Figure 2 and Table 2) yet exhibit the same sequential and medium-range NOE connectivities. This might be due to oxidation of Met 33 to methionine sulfoxide in a fraction of the SP-C molecules (Curstedt et al., 1990). This modification is probably inadvertant, since different batches of SP-C exhibited different relative populations of the two forms, with an abundance of 20%–50% of the species with the higher field amide proton resonance. This implicated covalent modification of Met 33 seems to slightly affect residues 28 and 30–32, for which two sets of nearly degenerate $^1H$ resonances are observed (Figure 2 and Table 2).

*Amide Proton Exchange in SP-C.* Inspection of the TOCSY and NOESY spectra recorded in $C^2HCl_3/C^2H_3O^2H$/0.1 M $^2HCl$ (Table 1) revealed that all amide protons in the polypeptide segment Leu 10–Leu 32 exchange slowly. The relative volumes of the αH–NH cross peaks of residues 10–11 and 30–32 were larger than 50% of those in the spectra recorded in $C^2HCl_3/C^2H_3OH$/0.1 M HCl, and for residues 12–29 these relative volumes were larger than 80%. From these estimates of the relative intensities, the $k_{NH}$ values in the legend to Figure 1 were derived. The amide protons of residues 1–9 and 33–35 had completely vanished already in the first spectrum recorded in the deuterated solvent; *i.e.*, the relative intensity must have been <5%.

*Three-Dimensional Structure Determination of SP-C.* Using an empirical pattern recognition approach (Wüthrich et al., 1984; Wüthrich, 1986), the combination of strong sequential $d_{NN}$ connectivities, observation of a significant number of $d_{\alpha N}(i,i+3)$, $d_{\alpha\beta}(i,i+3)$, and $d_{\alpha N}(i,i+4)$ connectivities, $^3J_{NH\alpha}$ coupling constants <5.0 Hz for all non-Gly residues in the polypeptide segment 8–35, and slowed amide proton exchange for residues 10–32 (Figure 1) indicates that SP-C forms a continuous α-helix comprising approximately residues 8–35. To obtain a more precise definition of the SP-C structure, we used the data of Figure 1 together with 132 intraresidual NOE distance constraints as input for a structure calculation with the distance geometry program DIANA. The complete input included 243 NOE upper distance constraints and 82 dihedral angle constraints (31 φ, 31 ψ, and 20 $\chi^1$) generated with the program HABAS from $^3J_{NH\alpha}$ and intraresidual and sequential NOE distance constraints (Güntert et al., 1989). Stereospecific assignments for 14 prochiral centers obtained with GLOMSA (See Table 2) were used in the final calculations. Since we did not observe any NOEs between the palmitoyl moieties and the polypeptide chain, the residues 5 and 6 were treated as cysteinyls in the calculations. Only one set of resonances for the residues 28 and 30–33 (Table 2) was used in the structure calculation, since identical NOEs were observed for the two species.

In the final round of structure calculations, 50 randomly generated starting conformations were subjected to DIANA minimization against the NMR input data. For all 50 calculations the residual NOE distance constraint violations were all smaller than 0.7 Å, the van der Waals violations were all smaller than 0.4 Å, and no dihedral angle constraints were significantly violated. The 20 structures with the smallest target functions were energy-minimized using the program OPAL, and the resulting group of 20 refined conformers is used to represent the three-dimensional structure of native SP-C in the organic solvent (Figure 5). Table 3 presents a survey of the parameters which afford a quantitative evaluation of the quality of the structure determination.

*Solution Structure of SP-C.* Inspection of the polypeptide backbone of the 20 energy-refined DIANA conformers after global superposition of the backbone atoms N, $C^{\alpha}$, and C′ of residues 7–34 for minimal RMSD (Figure 5) shows that residues 9–34 form a well-defined α-helix, while residues 1–8 and the C-terminal Leu 35 are flexibly disordered. The helical part of the structure is further characterized by the following observations: Calculation of local RMSDs (Figure 6) shows

Table 3: Quantitative Characterization of the 20 DIANA Conformers Used To Represent the Solution Structure of Native SP-C before and after Energy Minimization with the Program OPAL

| quantity | average value ± standard deviation (range) before energy minimization | after energy minimization |
|---|---|---|
| target function (Å²) | 0.36 ± 0.04 (0.27, ..., 0.42) | |
| AMBER energy (kcal/mol) | 32 ± 23 (−16, ..., 78) | −351 ± 13 (−375, ..., −325) |
| residual NOE distance constraint violations | | |
| number > 0.1 Å | 7.6 ± 1.4 (6.0, ..., 10.0) | 0.1 ± 0.2 (0.0, ..., 1.0) |
| sum (Å) | 3.0 ± 0.2 (2.7, ..., 3.4) | 4.5 ± 0.2 (4.2, ..., 4.8) |
| maximum (Å) | 0.20 ± 0.02 (0.19, ..., 0.23) | 0.09 ± 0.00 (0.09, ..., 0.10) |
| residual dihedral angle constraint violations | | |
| number > 2.5° | 0 | 0 |
| sum (deg) | 2.7 ± 1.1 (2.0, ..., 6.1) | 8.9 ± 1.6 (6.4, ..., 12.4) |
| maximum (deg) | 1.2 ± 0.5 (0.9, ..., 2.4) | 1.7 ± 0.1 (1.6, ..., 1.9) |
| RMSDs (Å)[a] | | |
| backbone N, Cα, C′ of residues 9–34 | 0.71 ± 0.23 (0.22, ..., 1.32) | 0.52 ± 0.16 (0.21, ..., 1.13) |
| all heavy atoms of residues 9–34 | 1.44 ± 0.25 (0.93, ..., 2.19) | 1.26 ± 0.22 (0.74, ..., 1.98) |
| backbone N, Cα, C′ of residues 19–29 | 0.04 ± 0.02 (0.00, ..., 0.09) | 0.08 ± 0.03 (0.02, ..., 0.15) |
| all heavy atoms of residues 19–29 | 0.28 ± 0.13 (0.01, ..., 0.47) | 0.11 ± 0.04 (0.03, ..., 0.21) |

[a] RMSD values are given with respect to the mean structure.

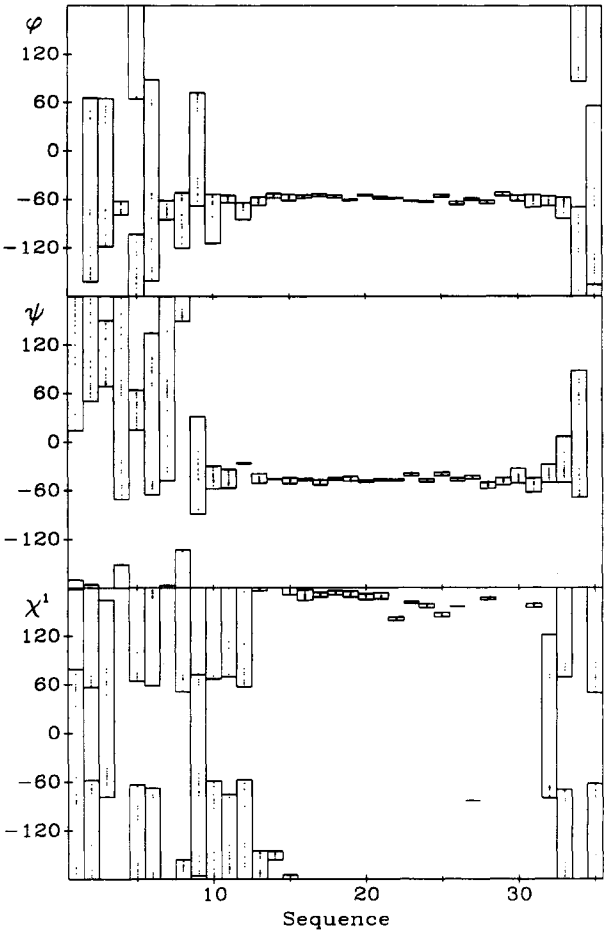


FIGURE 7: Plots of the $\varphi$, $\psi$, and $\chi^1$ dihedral angles *versus* the amino acid sequence of SP-C. In each plot the vertical bars span the range of values covered by the 20 conformers, and the dots represent the values in the 20 individual energy-minimized DIANA conformers.

that the polypeptide backbone conformation from residues 9–32 is very well-defined on the level of tripeptide segments, and for the amino acid side chains a high precision of the structure determination was achieved for residues 15–31, which includes the all-hydrophobic part of the helix (Figure 1). These results are confirmed by an analysis of the dihedral angles $\phi$, $\psi$, and $\chi^1$ (Figure 7). The $\phi$ and $\psi$ values in the 20 conformers cover virtually identical, very narrow ranges of values in the residues 10–33. Similarly, the $\chi^1$ angles of residues 14–28 and 31 are very precisely defined. Considering that, according

Table 4: Hydrogen Bonds Observed in the NMR Solution Structure of Native SP-C

| donor[a] | acceptor[a] | Nr[b] | donor[a] | acceptor[a] | Nr[b] |
|---|---|---|---|---|---|
| 8 Val NH | 6 Cys O′ | 13 | 24 Val NH* | 20 Val O′ | 20 |
| 13 Leu NH* | 9 Asn O′ | 17 | 25 Val NH* | 21 Val O′ | 20 |
| 14 Leu NH* | 10 Leu O′ | 16 | 26 Val NH* | 22 Leu O′ | 20 |
| 15 Val NH* | 11 Lys O′ | 16 | 27 Ile NH* | 23 Val O′ | 20 |
| 16 Val NH* | 12 Arg O′ | 20 | 28 Val NH* | 24 Val O′ | 20 |
| 17 Val NH* | 13 Leu O′ | 20 | 29 Gly NH* | 25 Val O′ | 20 |
| 18 Val NH* | 14 Leu O′ | 20 | 30 Ala NH(*) | 26 Val O′ | 20 |
| 19 Val NH* | 15 Val O′ | 20 | 31 Leu NH(*) | 27 Ile O′ | 20 |
| 20 Val NH* | 16 Val O′ | 19 | 32 Leu NH(*) | 28 Val O′ | 20 |
| 21 Val NH* | 17 Val O′ | 19 | 33 Met HN | 29 Gly O′ | 20 |
| 22 Leu NH* | 18 Val O′ | 20 | 34 Gly HN | 30 Ala O′ | 15 |
| 23 Val NH* | 19 Val O′ | 20 | | | |

[a] The criteria used for the identification of a hydrogen bond (Levitt, 1983) are that the proton–acceptor distance $d \leq 2.4$ Å and that the angle between the donor–proton bond and the line connecting the donor and acceptor heavy atoms ≤35° in at least 13 of the 20 conformers. In these two columns only those residues are listed which are, according to these criteria, involved in a hydrogen bond. Slow exchange was observed for the amide protons identified with an asterisk, and (*) indicates medium-slow exchange (Figure 1). [b] Number of conformers containing the hydrogen bond.

to the definition of the dihedral angle $\chi^1$ (IUPAC-IUB Commission on Biochemical Nomenclature, 1970), $\chi^1$(Val) = $\chi^1$(Ile) − 120°, the $\chi^1$ angles of all residues 15–28 are virtually identical. Finally, hydrogen bonds connecting the carbonyl oxygens and the amide protons of residues *i* and *i* + 4 were unambiguously identified in the entire polypeptide segment 9–34 (Table 4). The hydrophobic part of the SP-C helix is displayed in Figure 8, which confirms the picture of a highly regular, precisely defined α-helix. For the amino acid side chains the input of NOE distance constraints was scarce, and outside of the segment 14–31 the $\chi^1$ angles are correspondingly poorly defined. In the hydrophobic helical segment 15–28, the precise orientation of the side chains is probably largely due to the van der Waals constraints arising from the steric crowding by the branched Val side chains. The length of the α-helix, defined as the distance from the amide nitrogen of Asn 9 to the carbonyl carbon of Gly 34 is 37 Å, and the length of the all-aliphatic part from the amide nitrogen of Leu 13 to the carbonyl carbon of Val 28 is 23 Å. The distances from the γ-methyl protons of Val *i* to those of Val *i* + 2, which approximately correspond to the diameter of the helix in the central, hydrophobic segment, are about 10 Å.

*Stereospecific Assignments and Chemical Shifts of the Valyl Methyl Groups.* For the γ-methyl groups of the valyls

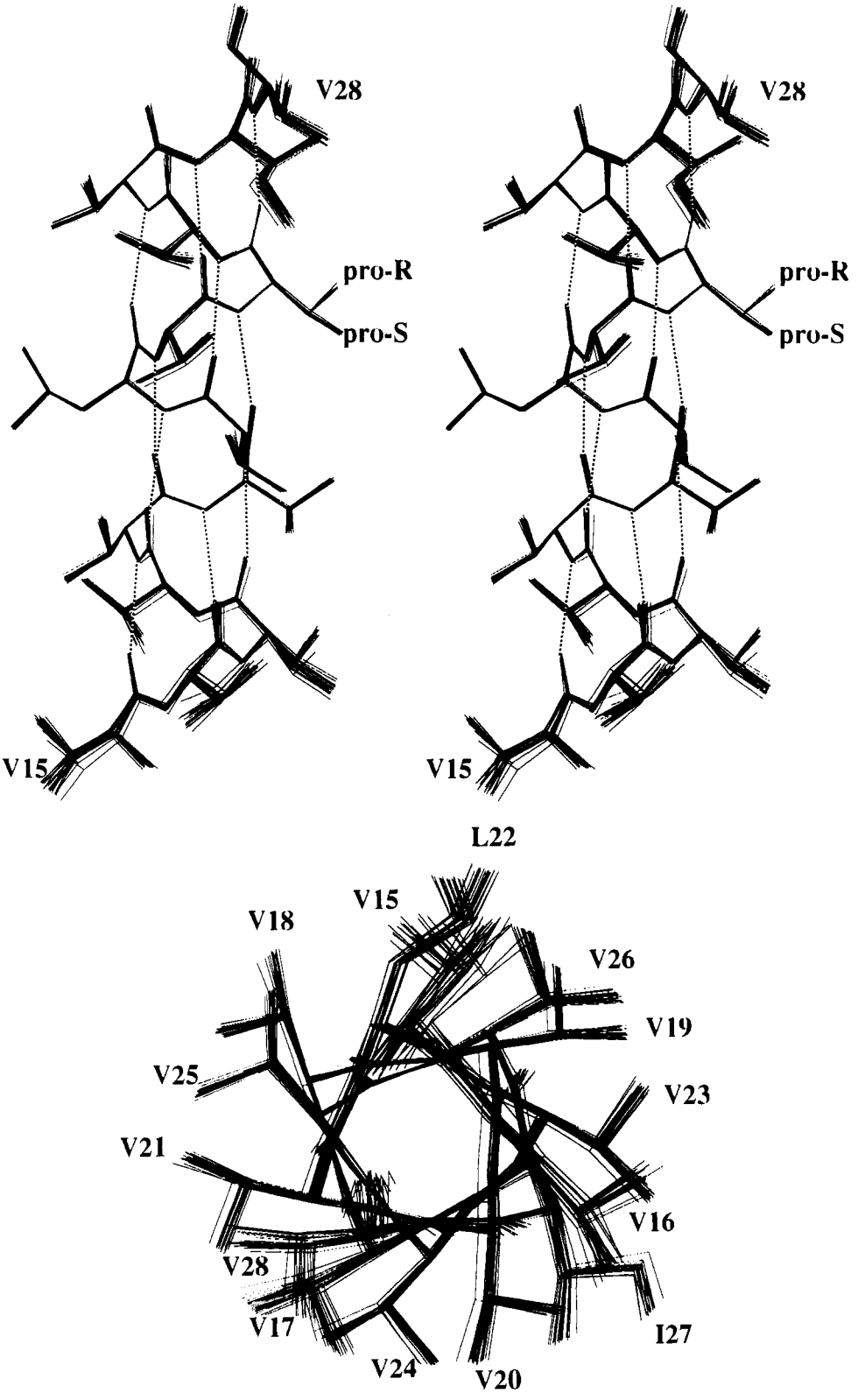


FIGURE 8: All-heavy-atom presentations for the segment 15–28 of the 20 energy-refined DIANA conformers of SP-C. (A, top) Stereoview perpendicular to the helix axis. For Val 24 the *pro-R* and *pro-S* γ-methyl groups are also labeled. Hydrogen bonds (Table 4) are drawn as dotted lines. (B, bottom) View along the helix axis. All side chains are identified with the one-letter amino acid code and the sequence location. In both drawings the conformers 2–20 were superimposed with conformer 1 for pairwise minimal RMSD of the backbone atoms N, $C^{\alpha}$, and C′.

15, 16, 18, 21, 23, 25, 26, and 28 a sufficient number of NMR constraints was available to obtain stereospecific assignments using the program GLOMSA. In all these residues, the *pro-S* ($\gamma^2$) methyl group exhibits a lower field $^1H$ chemical shift than the *pro-R* methyl group (Figure 9a and Table 2). Of the four valyls 17, 19, 20, and 24, for which no stereospecific assignments could be obtained, the intensities of the intraresidual NOESY cross peaks with the amide proton are clearly larger for the peaks involving the methyl group with the lower field chemical shift (Figure 9B). Since, as was to be expected for a highly regular α-helical structure in an isotropic solvent, the γ-methyl chemical shifts from Val 15

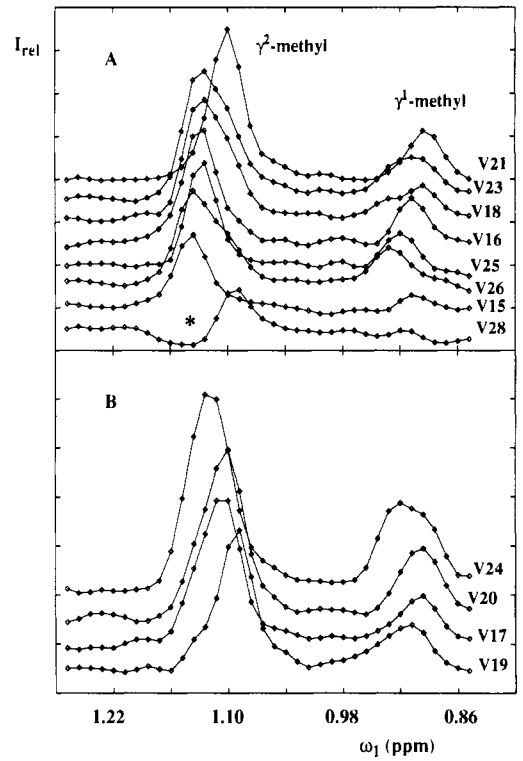


FIGURE 9: Cross sections along $\omega_1$ showing the relative intensities, $I_{rel}$, of the intraresidual NOESY cross peaks between the amide protons and the $\gamma$-methyls of Val. The cross sections were taken from the NOESY spectrum shown in Figures 3 and 4 at the $\omega_2$ frequencies of the amide protons (see Figure 2). (A) Val residues for which stereospecific assignments of the $\gamma^1$- and $\gamma^2$-methyl groups were obtained with GLOMSA. The asterisk above the trace for Val 28 indicates a negative ridge along $\omega_2$ caused by the methyl groups of the other valyl residues. (B) Val residues for which insufficient data were available for obtaining stereospecific assignments.

to Val 28 are very similar (Figures 2 and 9, Table 2), this suggests that for all valyls in the helix the *pro-S* methyl group is, by its location closer to the amide group (Figure 8A), downfield-shifted relative to the *pro-R* methyl group. This clear-cut correlation between configuration and chemical shift of the diastereotopic methyls in the valyl residues can be rationalized along the same lines as the near-identity of the chemical shifts of the nonlabile protons of all valyls in the SP-C helix, *i.e.*, by the pronounced periodicity of the molecular structure and its solvent environment. In globular proteins, irregularities of the secondary structures and their aperiodic environment tend to further affect the chemical shifts (Neri et al., 1990). In general, therefore, stereospecific assignments of methyl groups cannot be based on the chemical shifts alone but have to rely either on global structure analyses, as implemented in GLOMSA (Güntert et al., 1991b), or on biochemical methods (Neri et al., 1989; Szyperski et al., 1992b).

*General Considerations on Conformational Polymorphism of SP-C.* Val residues are in general underrepresented in $\alpha$-helices and overrepresented in $\beta$-sheets (Levitt, 1978). Accordingly, secondary-structure predictions of SP-C, *e.g.*, with the algorithm of Chou & Fasman (1974), yield exclusively $\beta$-sheet structures. Val occurs also less frequently in transmembrane helices than Leu (von Heijne & Gavel, 1988), which has a higher $\alpha$-helical propensity than Val. The presently observed $\alpha$-helical structure of SP-C might thus represent a thermodynamically metastable state; this appears to be supported by the fact that the monomeric helical form was observed only in freshly prepared solutions. Others have reported that full-length SP-C polypeptides exhibit different conformations depending on the palmitoylation status, with the non-palmitoylated dimeric molecules forming preferentially $\beta$-sheet structures (Baatz et al., 1992; Pastrana et al., 1991; Vandenbussche et al., 1992). However, the solvent environment appears to have a strong influence as well. The NMR-derived secondary structure in dodecylphosphocholine micelles of a synthetic peptide corresponding to the sequence 1–17 of SP-C includes a helix from residues 11–17, although the cysteinyls at positions 5 and 6 are not acylated (J. Johansson, T. Szyperski, and K. Wüthrich, to be published). These observations with SP-C coincide with earlier studies of water-soluble block copolymers of D,L-Lys and L-Val, where a -($Val_{15}$)- block was found to be ~50% $\alpha$-helical in 98% aqueous methanol, but to form dimeric $\beta$-structure in water (Epand & Scheraga, 1968).

*Structure and Physiological Functions of SP-C.* The pronounced hydrophobicity of SP-C makes large-scale production difficult. Thus, protein-containing surfactant preparations used for treatment of RDS are still predominantly derived from natural sources (Robertson et al., 1992). From the presently described investigation, we now know that the length of the SP-C $\alpha$-helix is optimally suited for interacting with DPPC bilayers in the liquid-crystalline phase but is too short to span gel-phase bilayers. A study using scanning calorimetry demonstrated that mismatches between the length of simplified membrane-spanning helical peptides and the phospholipid bilayer with which they interact may cause phase separation of peptides and lipids if the peptide is shorter than the thickness of the lipid bilayer (Zhang et al., 1992). Thus, from its structure it seems likely that SP-C is preferentially present in fluid surfactant DPPC bilayers. This is also supported by a recent fluorescence energy-transfer study (Horowitz et al., 1993), which showed that gel-phase phospholipid bilayers induce aggregation of SP-C polypeptides. Overall, it thus appears quite likely that the function of SP-C is primarily governed by the overall length of its folded form. Accordingly, useful SP-C substitutes might be obtained in the form of analogs with conformational features similar to those presented here for SP-C, which might, however, have covalent structures that are better suited for large-scale production of exogenous surfactant to be used in RDS therapy.

## ACKNOWLEDGMENT

We thank R. Marani for the careful processing of the manuscript.

## REFERENCES

Anil-Kumar, Ernst, R. R., & Wüthrich, K. (1980) *Biochem. Biophys. Res. Commun. 95*, 1–6.

Baatz, J. E., Smyth, K. L., Whitsett, J. A., Baxter, C., & Absolom, D. R. (1992) *Chem. Phys. Lipids 63*, 91–104.

Billeter, M., Schaumann, T., Braun, W., & Wüthrich, K. (1990) *Biopolymers 29*, 695–706.

Bothner-By, A. A., Stephens, R. L., Lee, J., Warren, C. D., & Jeanloz, R. W. (1984) *J. Am. Chem. Soc. 106*, 811–813.

Chou, P. Y., & Fasman, G. D. (1974) *Biochemistry 13*, 222–245.

Collaborative European Multicenter Study Group (1988) *Pediatrics 82*, 683–691.

Curstedt, T., Jörnvall, H., Robertson, B., Bergman, T., & Berggren, P. (1987) *Eur. J. Biochem. 168*, 255–262.

Curstedt, T., Johansson, J., Persson, P., Eklund, A., Robertson, B., Löwenadler, B., & Jörnvall, H. (1990) *Proc. Natl. Acad. Sci. U.S.A. 87*, 2985–2989.

DeMarco, A., & Wüthrich, K. (1976) *J. Magn. Reson. 24*, 201–204.

Eccles, C., Güntert, P., Billeter, M., & Wüthrich, K. (1991) *J. Biomol. NMR 1*, 111–130.
Epand, R. F., & Scheraga, H. A. (1968) *Biopolymers 6*, 1551–1571.
Griesinger, C., Otting, G., Wüthrich, K., & Ernst, R. R. (1988) *J. Am. Chem. Soc. 110*, 7870–7882.
Güntert, P., & Wüthrich, K. (1991) *J. Biomol. NMR 1*, 447–456.
Güntert, P., & Wüthrich, K. (1992) *J. Magn. Reson. 96*, 403–407.
Güntert, P., Braun, W., Billeter, M., & Wüthrich, K. (1989) *J. Am. Chem. Soc. 111*, 3997–4004.
Güntert, P., Braun, W., & Wüthrich, K. (1991a) *J. Mol. Biol. 217*, 517–530.
Güntert, P., Qian, Y. Q., Otting, G., Müller, M., Gehring, W., & Wüthrich, K. (1991b) *J. Mol. Biol. 217*, 531–540.
Güntert, P., Dötsch, V., Wider, G., & Wüthrich, K. (1992) *J. Biomol. NMR 2*, 619–629.
Hawgood, S., Benson, B. J., Schilling, J., Damm, D., Clements, J. A., & White, R. T. (1987) *Proc. Natl. Acad. Sci. U.S.A. 84*, 66–70.
Horowitz, A. D., Elledge, B., Whitsett, J. A., & Baatz, J. E. (1992) *Biochim. Biophys. Acta 1107*, 44–54.
Horowitz, A. D., Baatz, J. E., & Whitsett, J. A. (1993) *Biochemistry 32*, 9513–9523.
IUPAC-IUB Commission on Biochemical Nomenclature (1970) *Biochemistry 9*, 3471–3479.
Johansson, J., Curstedt, T., Robertson, B., & Jörnvall, H. (1988a) *Biochemistry 27*, 3544–3547.
Johansson, J., Jörnvall, H., Eklund, A., Christensen, N., Robertson, B., & Curstedt, T. (1988b) *FEBS Lett. 232*, 61–64.
Johansson, J., Persson, P., Löwenadler, B., Robertson, B., Jörnvall, H., & Curstedt, T. (1991) *FEBS Lett. 281*, 119–122.
Johansson, J., Curstedt, T., & Robertson, B. (1994) *Eur. Respir. J. 7*, 372–391.
Levitt, M. (1978) *Biochemistry 17*, 4277–4285.
Levitt, M. (1983) *J. Mol. Biol. 170*, 723–764.
Liu, Y., Fisher, D. A., & Storm, D. R. (1993) *Biochemistry 32*, 10714–10719.
Marion, D., Ikura, M., & Bax, A. (1989a) *J. Magn. Reson. 84*, 425–430.
Marion, D., Ikura, M., Tschudin, R., & Bax, A. (1989b) *J. Magn. Reson. 85*, 393–399.
Morrow, M. R., Taneva, S., Simatos, G. A., Allwood, L. A., & Keough, K. M. W. (1993) *Biochemistry 32*, 11338–11344.
Neri, D., Szyperski, T., Otting, G., Senn, H., & Wüthrich, K. (1989) *Biochemistry 28*, 7510–7516.
Neri, D., Otting, G., & Wüthrich, K. (1990) *Tetrahedron 46*, 3287–3296.
Oosterlaken-Dijksterhuis, M. A., Haagsman, H. P., van Golde, L. M. G., & Demel, R. A. (1991a) *Biochemistry 30*, 8276–8281.
Oosterlaken-Dijksterhuis, M. A., Haagsman, H. P., van Golde, L. M. G., & Demel, R. A. (1991b) *Biochemistry 30*, 10965–10971.
Pastrana, B., Mautone, A. J., & Mendelsohn, R. (1991) *Biochemistry 30*, 10058–10064.
Rance, M., Sørensen, O. W., Bodenhausen, G., Wagner, G., Ernst, R. R., & Wüthrich, K. (1983) *Biochem. Biophys. Res. Commun. 117*, 479–485.
Robertson, B., van Golde, L. M. G., & Batenburg, J. J., Eds. (1992) in *Pulmonary Surfactant. From Molecular Biology to Clinical Practice*, Elsevier, Amsterdam, The Netherlands.
Simatos, G. A., Forward, K. B., Morrow, M. R., & Keough, K. M. W. (1990) *Biochemistry 29*, 5807–5814.
Szyperski, T., Güntert, P., Otting, G., & Wüthrich, K. (1992a) *J. Magn. Reson. 99*, 552–560.
Szyperski, T., Neri, D., Leiting, B., Otting, G., & Würthrich, K. (1992b) *J. Biomol. NMR 2*, 323–334.
Vandenbussche, G., Clercx, A., Curstedt, T., Johansson, J., Jörnvall, H., & Ruysschaert, J. M. (1992) *Eur. J. Biochem. 203*, 201–209.
von Heijne, G., & Gavel, Y. (1988) *Eur. J. Biochem. 174*, 671–678.
Weiner, S. J., Kollman, P. A., Nguyen, D. T., & Case, D. A. (1986) *J. Comput. Chem. 7*, 230–252.
Wüthrich, K. (1986) in *NMR of Proteins and Nucleic Acids*, Wiley, New York.
Wüthrich, K., Billeter, M., & Braun, W. (1984) *J. Mol. Biol. 180*, 715–740.
Xia, T. H. (1992) Ph.D. Thesis Nr. 9831, ETH Zürich, Switzerland.
Yu, S. H., & Possmayer, F. (1990) *Biochim. Biophys. Acta 1046*, 233–241.
Zhang, Y. P., Lewis, R. N. A. H., Hodges, R. S., & McElhaney, R. N. (1992) *Biochemistry 31*, 11579–11588.